

Rodrigues, A.E., Lu, Z.P., Loureiro, J.M., and **Pais** L.S.

Modeling and Operation of a Simulated Moving Bed for the Separation of Optical Isomers

Fundamentals of Adsorption 5, M.D. LeVan (ed.), Kluwer Academic Publishers, Boston, Massachusetts, p. 765-772 (1996).

Fundamentals of Adsorption

M.D. LeVan (ed.), Kluwer Academic Publishers
Boston, Massachusetts, 1996

Modeling and Operation of a Simulated Moving Bed for the Separation of Optical Isomers

A.E. Rodrigues*, J.M. Loureiro, Z.P. Lu and L.S. Pais
Laboratory of Separation and Reaction Engineering
School of Engineering, University of Porto
4099 Porto Codex, Portugal

Abstract. A model for predicting the steady state behavior of the simulated moving bed (SMB) is developed. SMB performance is characterized by purity, recovery, solvent consumption and productivity. The effect of switching time (rotation period), extract flowrate and section length on the SMB performance is discussed. A pilot plant for the separation of optical isomers is operated and tested with two systems: "Sandoz epoxide" and "bi-naphthol".

INTRODUCTION

The simulated moving bed (SMB) technology developed by UOP [1-3] has been used in chemical industry in various applications such as the recovery of p-xylene (Parex process) and the separation glucose/fructose (Sarex process) [3,4]. However, the use of SMB in the field of pharmaceuticals and fine chemistry is new. Pilot and industrial SMB for such applications have been recently developed by SEPAREx [5].

The separation of enantiomers is an important issue in various areas and particularly in the health-related field. It is well known that isomers can have different therapeutic value and there is pressure of regulatory agencies to the separation of isomers [6]. Separation by conventional techniques is difficult because separation factors are low and therefore SMB technology is appropriate provided chromatographic phases for enantiomer separation are available [7,8].

The objectives of this work are i) to develop a model to predict the effect of operating variables (flowrates, rotation period, section length) on the process performance; and ii) to operate the SMB pilot plant with two test systems (Sandoz epoxide and bi-naphthol).

MODEL DEVELOPMENT

The simulated moving bed can be represented by two different models: the true SMB and the steady state true moving bed, TMB. Since these two systems have similar performances, and the TMB approach requires shorter computation times, we can simulate and obtain the optimum operating conditions for the SMB, using the TMB model [9-16].

The cyclic behavior of the simulated moving bed can be calculated from the steady state model of the true moving bed, taking into account the relation between the solid velocity u_s and the rotation period (or switching time) ΔT , $u_s = L_c / \Delta T$ where L_c is the column length.

The equivalence between the SMB and its corresponding TMB is made by keeping constant the liquid velocity relative to the solid velocity (both in centimeters of column per second): $v_j^{SMB} = v_j^{TMB} + u_s$, where v_j is the interstitial fluid velocity in the j section of the moving bed.

Model equations

In the steady state model developed for the TMB simulation, axial dispersed plug flow of the fluid phase and mass transfer rate simulated by the linear driving force (LDF) approximation are assumed and the multicomponent adsorption equilibrium is taken into account.

Model equations are the mass balances in a volume element of the bed and in the solid with the respective boundary conditions:

$$\varepsilon D_{Lj} \frac{d^2 c_{ij}}{dz^2} - \varepsilon v_j \frac{dc_{ij}}{dz} + (1 - \varepsilon) u_s \frac{dq_{ij}}{dz} = 0 \quad (1)$$

$$u_s \frac{dq_{ij}}{dz} + k [f(c_{ij}) - q_{ij}] = 0 \quad (2)$$

The boundary conditions for section j are:

$$z = 0 \quad c_{ij} - \frac{D_{Lj}}{v_j} \frac{dc_{ij}}{dz} = c_{ij,0} \quad (3a)$$

$$z = L_j \quad \frac{dc_{ij}}{dz} = 0 \quad \text{and} \quad q_{ij} = q_{ij+1,0} \quad (3b)$$

Multicomponent adsorption isotherm:

$$f(c_{ij}) = k_i c_{ij} + \frac{q_m b_i c_{ij}}{1 + \sum b_i c_{ij}} \quad (4)$$

In the above equations c_{ij} and q_{ij} are the concentrations of species i ($i=1,2$) in the fluid and solid phases respectively in section j ($j=1,2,3,4$) of the TMB and k is the mass transfer coefficient for the LDF approximation.

The boundary conditions (eqs 3a-3b) depend on the TMB section j , since the fluid phase flows from one section to another; the following mass balances at the nodes of the TMB identify the section j under consideration and should be substituted in eq 3a according to j :

$$\text{Eluent node (j=1):} \quad c_{i1,0} = \frac{v_4}{v_1} c_{i4,L4} \quad (5a)$$

$$\text{Extract node (j=2):} \quad c_{i2,0} = c_{i1,L_1} \quad (5b)$$

$$\text{Feed node (j=3):} \quad c_{i3,0} = \frac{v_2}{v_3} c_{i2,L_2} + \frac{v_F}{v_3} c_i^F \quad (5c)$$

$$\text{Raffinate node (j=4):} \quad c_{i4,0} = c_{i3,L_3} \quad (5d)$$

Introducing the dimensionless space variable $x = z/L_j$ and $\tau_s = L_j/u_s = N_s \Delta T$, the model parameters are the Peclet number $Pe_j = v_j L_j / D_{Lj}$, the ratio between fluid and solid velocities $\gamma_j = v_j / u_s$, the number of mass transfer units $\alpha_j = k L_j / u_s$, and the ratio between the solid and fluid volumes $(1 - \varepsilon) / \varepsilon$.

SIMULATION RESULTS

Model equations were numerically solved by using the method of orthogonal collocation in finite elements. The effects of the rotation period, extract flowrate, and number of columns in the SMB performance were studied by simulation.

Performance parameters were defined, based on a two component separation in the SMB, considering that the less retained species A is recovered in the raffinate, while the more retained component B is recovered in the extract.

Purity (%) for the extract, PUX (raffinate, PUR) are defined as the ratio between the concentration of the more (less) retained component and the total concentration of the two enantiomers in the extract (raffinate), i.e., $PUX = 100 C_X^B / (C_X^A + C_X^B)$ and $PUR = 100 C_R^A / (C_R^A + C_R^B)$.

The recovery (%) RCX (RCR) is the ratio between the amount of the strong (weak) retained component in the extract (raffinate), and the amount of the same component in the feed, $RCX = 100 C_X^B Q_X / C_F^B Q_F$ and $RCR = 100 C_R^A Q_R / C_F^A Q_F$.

The solvent consumption (l/g) SCX (SCR) in the production of the strong (weak) retained component is the total amount of solvent necessary to produce one gram of the strong (weak) retained component, i.e., $SCX = (Q_E + Q_F) / C_X^B Q_X$ and $SCR = (Q_E + Q_F) / C_R^A Q_R$.

The productivity (g/hr/l of solid) PRX (PRR) is the amount of the more (less) retained component obtained in the extract (raffinate) per liter of stationary phase per hour, i.e., $PRX = C_X^B Q_X / V_s$ and $PRR = C_R^A Q_R / V_s$.

If the separation of enantiomers in a racemic mixture is considered, $C_F^A = C_F^B$ and then $SCX = SCR \cdot RCR / RCX$ and $PRX = PRR \cdot RCX / RCR$.

The separation of enantiomers of 1a,2,7,7a-tetrahydro-3-methoxynaphta-(2,3b)-oxirane (Sandoz epoxide) in cellulose triacetate columns using methanol as eluent [17,18,19] was studied. The adsorption equilibrium isotherm proposed by Nicoud *et al.* [17] was used:

$$f_i(c_i, c_j) = k_i c_i + \frac{q_m b_i c_i}{1 + b_i c_i + b_j c_j} \quad (6)$$

with $k_A = k_B = 1.57$, $q_m = 5.8$ g/l, $b_A = 0.045$ l/g and $b_B = 0.127$ l/g.

A reference case, based on the values of operating variables and model parameters shown in Table 1, was chosen and the influence of several operating variables was studied by simulation. The internal profiles for the reference case are shown in figure 1.

Table 1. Operating conditions and model parameters for the reference case.

SMB operation conditions		Model parameters	
Feed concentration:	5 g/l each	Solid/fluid volumes, $(1-\epsilon)/\epsilon = 1.5$	
Rotation Period:	248 sec	No. mass transfer units, $\alpha = 74.4$	
Recycling Flowrate:	20.35 ml/min	Peclet Number, $Pe = 2000$	
Eluent Flowrate:	4.53 ml/min		
Extract Flowrate:	4.00 ml/min	Columns	
Feed Flowrate:	1.52 ml/min	Diameter:	2.6 cm
Raffinate Flowrate:	2.05 ml/min	Section Length:	33.0 cm

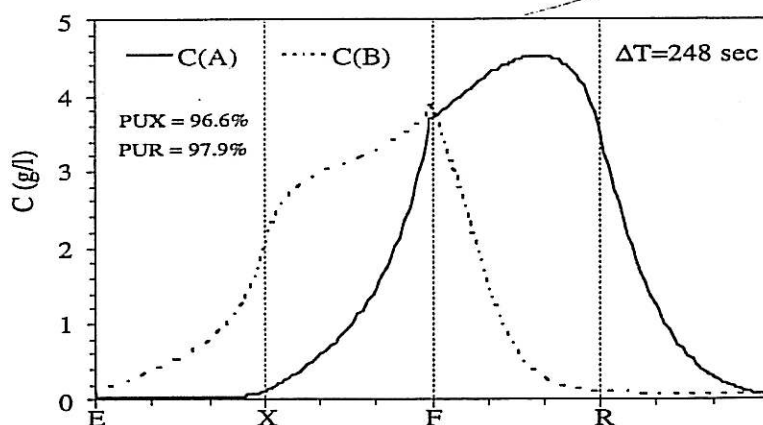


Figure 1. Internal profiles for the reference case.

The influence of the rotation period on the system performance is shown in figure 2. It can be seen that high purities can be obtained only in a narrow window of rotation periods.

The effect of the extract flowrate on the SMB performance is shown in figure 3. Depending on the sense of variation, the deviation of the extract flowrate from its optimum value drastically affects the performance for one or the other enantiomer. Again, high purities for both enantiomers can be obtained only in a quite narrow window of values of the extract flowrate.

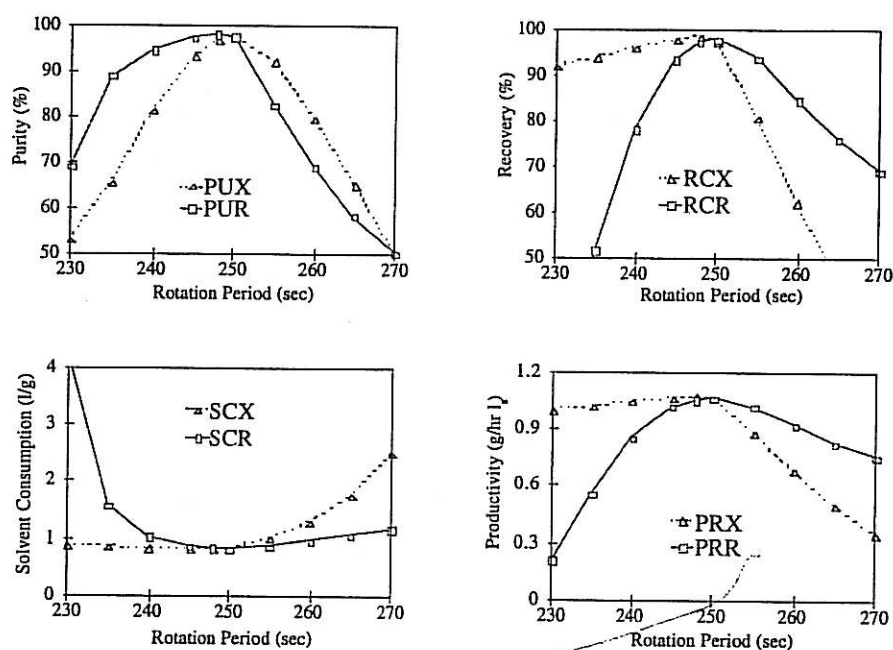


Figure 2. Influence of the rotation period on the performance parameters.

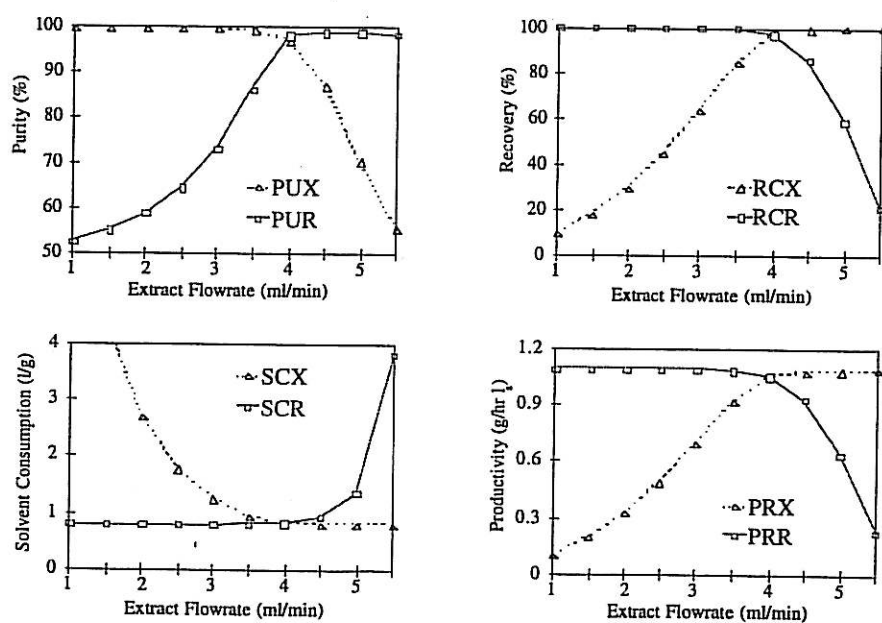


Figure 3. Effect of the extract flowrate on the performance parameters.

The effect of the section length is displayed in figure 4. With the mass transfer coefficient used ($k = 0.1 \text{ s}^{-1}$), no significant improvement in the system performance is observed for section length greater than 30 cm.

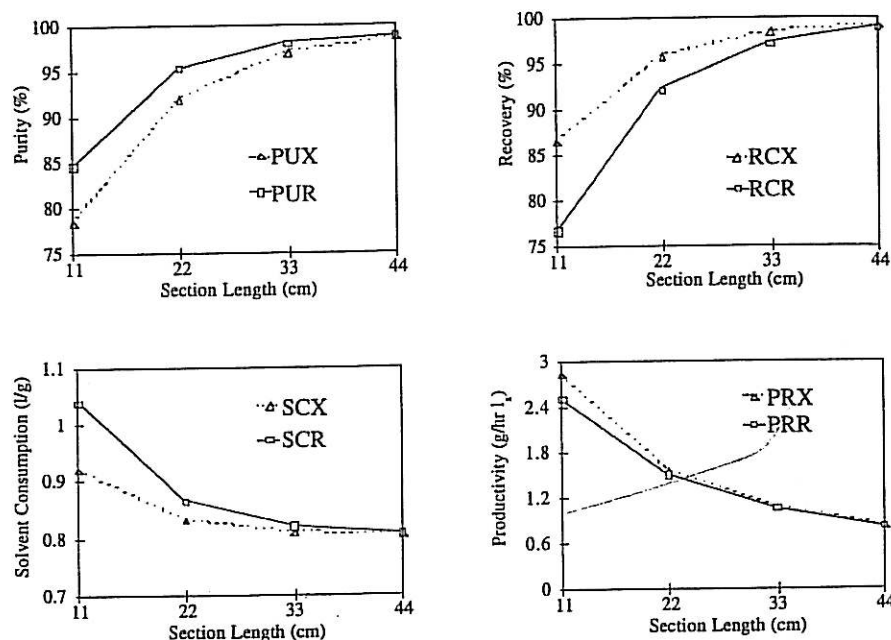


Figure 4. Effect of the section length on the performance parameters.

OPERATION OF SIMULATED MOVING BED

Preliminary runs of the pilot SMB were made for the Sandoz epoxide system. Due to high pressure drop in CTA columns, only a 4 columns configuration could be used. The purities achieved were 55% for the extract and 59% for the raffinate.

The separation of 1,1'-bi-2-naphtol enantiomers using 3,5-dinitrobenzoyl phenylglycine covalently bonded to silica gel as stationary phase and 72/28 (v/v) heptane-isopropanol as eluent was also studied. Purities of 94.4% for the extract and 98.9% for the raffinate were experimentally obtained with an 8-columns configuration SMB. Table 2 presents the experimental conditions for these two systems.

Simulation of the experimental run for the bi-naphtol system was done using the steady state TMB model presented before. A reasonable agreement is obtained between the experimental (symbols) and simulated (lines) results, shown in Figure 5.

Open symbols represent the instantaneous internal profiles collected at half-time of each rotation period. Black symbols represent the average concentration of the two components in the extract and raffinate, collected during a whole cycle.

The value for the mass transfer coefficient used in simulation was $k = 0.1 \text{ s}^{-1}$ and was estimated from experimental runs of adsorption/desorption in a single column.

Table 2. Experimental conditions for the test systems.

System:	Epoxide	Bi-naphtol
Column length, cm	8.6	10.5
Number of columns	4	8
Feed concentration, g/l each	0.5	2.9
Rotation Period, sec	235	170.4
Recycling flowrate, ml/min	20.10	35.38
Eluent flowrate, ml/min	3.90	21.45
Extract flowrate, ml/min	2.62	17.98
Feed flowrate, ml/min	1.00	3.64
Raffinate flowrate, ml/min	2.28	7.11

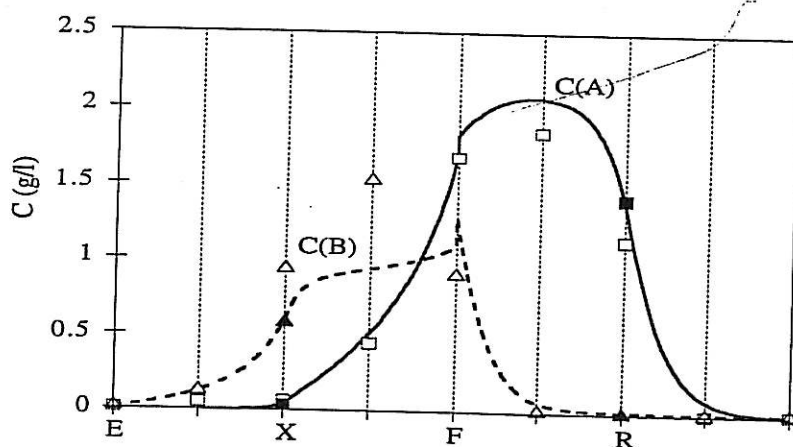


Figure 5. Experimental and model results for the Bi-naphtol system ($N_c=8$).

CONCLUSIONS

The simulated moving bed is modeled through the equivalent steady state true moving bed; this model is solved using the method of orthogonal collocation in finite elements; the effects of switching time (rotation period), extract flowrate and section length are studied by simulation.

A pilot plant SMB (using four and eight columns) is operated with two test systems: separation of Sandoz epoxide and separation of bi-naphtol enantiomers from racemic mixtures.

The model results in terms of internal profiles and performance (purities, recoveries and productivities of extract and raffinate and the respective solvent consumptions) agree fairly well with the experimental results.

REFERENCES

1. D.B. Broughton, U.S. Patent 2,985,589 (1961).
2. D.B. Broughton, Sep. Sci. Tech., 19, 723-736 (1984).
3. A.J. de Rosset, R.W. Neuzil, D.B. Broughton in A.E. Rodrigues and D. Tondeur, Percolation Processes: Theory and Applications, Sijthoff & Noordhoff, 1981.
4. K. Hashimoto, S. Adachi, H. Noujima and A. Maruyama, J. Chem. Eng. Jpn, 16, 400-406 (1983).
5. R. Nicoud, LC-GC Int., 5, 43-47 (1992).
6. R. Sheldon, Chirotechnology, M. Dekker, New York, 1993.
7. M. Negawa and F. Shoji, J. Chromatography, 590, 113-117 (1992).
8. R.M. Nicoud (Ed.), Simulated Moving Bed: Basics and Applications European Meeting, Nancy, Dec. 6th, 1993.
9. K.H. Chu and M.A. Hashim, The Chem. Eng. J., 56, 59-65 (1995).
10. M.M. Hassan, A.K. Rahman and K.F. Loughlin, Separations Technology, 4 (1), 15-26 (1994).
11. A.K. Rahman, M.M. Hassan and K.F. Loughlin, Separations Technology, 4 (1), 27-37 (1994).
12. K. Hidajat, C. Ching and D. Ruthven, Chem. Eng. Sci., 41, 2953-2956 (1986).
13. D. Ruthven and C. Ching, Chem. Eng. Sci., 44, 1011-1038 (1989).
14. G. Storti, M. Masi, S. Carra and M. Morbidelli, Chem. Eng. Sci., 44, 1329-1345 (1989).
15. G. Storti, M. Masi and M. Morbidelli in G. Ganetsos and P. Barker (Ed.), Preparative and Production Scale Chromatography, M. Dekker, New York, 1993, pp. 673-700.
16. B. Balannec and G. Hotier in G. Ganetsos and P. Barker (Ed.), Preparative and Production Scale Chromatography, M. Dekker, New York, 1993, pp. 301-357.
17. R.M. Nicoud, G. Fuchs, E. Kusters, R. Reuille and E. Schmid, 3rd Int. Symp. on Chiral Discrimination, Tübingen, Germany, Oct. 5-8, 1992.
18. A.E. Rodrigues, Z.P. Lu, J.M. Loureiro and L.S. Pais, J. Chromatogr. A, 702, 223-231 (1995).
19. G. Fuchs, R.M. Nicoud, and M. Bailly in M. Perrut (Ed.), Proceedings of the 9th Int. Symp. on Prep. and Ind. Chromatogr., Soc. Française de Chimie, 1992.